The EMBO Journal (2006) 25, 3000–3011 | © 2006 European Molecular Biology Organization | All Rights Reserved 0261-4189/06
www.embojournal.org

THE EMBO JOURNAL

Genetic linkage of *pfmdr1* with food vacuolar solute import in *Plasmodium falciparum*

Petra Rohrbach[1], Cecilia P Sanchez[1], Karen Hayton[2], Oliver Friedrich[3], Jigar Patel[4], Amar Bir Singh Sidhu[5], Michael T Ferdig[4], David A Fidock[5] and Michael Lanzer[1,*]

[1]Hygiene Institut, Abteilung Parasitologie, Universitätsklinikum Heidelberg, Heidelberg, Germany, [2]Laboratory of Malaria and Vector Research, National Institute of Allergy and Infectious Diseases, National Institutes of Health, Bethesda, MD, USA, [3]Medical Biophysics, Institute of Physiology and Pathophysiology, University of Heidelberg, Heidelberg, Germany, [4]Department of Biological Sciences, University of Notre Dame, IN, USA and [5]Department of Microbiology and Immunology, Albert Einstein College of Medicine, Bronx, NY, USA

The P-glycoprotein homolog of the human malaria parasite *Plasmodium falciparum* (Pgh-1) has been implicated in decreased susceptibility to several antimalarial drugs, including quinine, mefloquine and artemisinin. Pgh-1 mainly resides within the parasite's food vacuolar membrane. Here, we describe a surrogate assay for Pgh-1 function based on the subcellular distribution of Fluo-4 acetoxymethylester and its free fluorochrome. We identified two distinct Fluo-4 staining phenotypes: preferential staining of the food vacuole versus a more diffuse staining of the entire parasite. Genetic, positional cloning and pharmacological data causatively link the food vacuolar Fluo-4 phenotype to those Pgh-1 variants that are associated with altered drug responses. On the basis of our data, we propose that Pgh-1 imports solutes, including certain antimalarial drugs, into the parasite's food vacuole. The implications of our findings for drug resistance mechanisms and testing are discussed.

The EMBO Journal (2006) **25,** 3000–3011. doi:10.1038/sj.emboj.7601203; Published online 22 June 2006
Subject Categories: membranes & transport; microbiology & pathogens
Keywords: drug transport; Fluo-4; malaria; P-glycoprotein

Introduction

Many developing countries are engaged in a battle against malaria, an infectious disease that is endemic throughout most of Africa, Southeast Asia and Latin America, where it causes an estimated 515 million clinical cases annually (Snow *et al*, 2005). Options to control the spread of malaria are increasingly limited as widely used antimalarials are losing their efficacy, including the 4-aminoquinoline drug chloroquine and the folate antagonists pyrimethamine and sulfadoxine (Baird, 2005). Moreover, reduced susceptibility has emerged to other antimalarials, including quinine, mefloquine, and possibly artemether (Baird, 2005; Jambou *et al*, 2005).

In both microorganisms and tumors, drug resistance can arise from the presence of P-glycoproteins (P-gp) that are capable of extruding a broad range of structurally and functionally unrelated cytotoxic agents (Borges-Walmsley *et al*, 2003). P-gp belong to the ABC (ATP-binding cassette) transporter superfamily and are encoded by *mdr* genes. The human malaria parasite *Plasmodium falciparum* possesses an *mdr* homologue (*pfmdr1*) whose gene product, Pgh-1, is expressed during intraerythrocytic development of the parasite (Foote *et al*, 1989; Wilson *et al*, 1989). Pgh-1 has a domain structure typical of P-gp, with two homologous domains, each comprising a hydrophobic membrane-associated segment with six transmembrane domains followed by a hydrophilic nucleotide binding fold. Pgh-1 is mainly localized to the membrane of the parasite's acidic food vacuole (Cowman *et al*, 1991; Cremer *et al*, 1995), with its ATP binding domain facing the cytoplasm (Cowman *et al*, 1991; Karcz *et al*, 1993).

pfmdr1 has been implicated in several drug resistance phenotypes. For example, a comprehensive clinical study has shown a strong association between *pfmdr1* amplification and mefloquine treatment failure and *in vitro* resistance (Price *et al*, 2004). *pfmdr1* amplification is further associated with *in vitro* resistance to halofantrine and quinine (Wilson *et al*, 1993; Cowman *et al*, 1994). Furthermore, polymorphisms at amino-acid residues 86, 184, 1034, 1042 and 1246 have been associated with altered *in vitro* susceptibility to chloroquine, quinine, mefloquine and artemisinin (Duraisingh *et al*, 2000; Reed *et al*, 2000; Ngo *et al*, 2003; Pickard *et al*, 2003; Sidhu *et al*, 2005). In particular, the $N^{1042}D$ substitution seems to play a prominent role in low-level quinine resistance (Sidhu *et al*, 2005), while the $N^{86}Y$ substitution has been implicated in contributing to lumefantrine and high level chloroquine resistance (Duraisingh and Cowman, 2005; Sisowath *et al*, 2005). How Pgh-1 affects drug phenotypes is largely unclear. Pgh-1 may directly transport drugs, either out of or into the food vacuole, or alternatively, Pgh-1 may indirectly influence drug partitioning as a result of altered transport of other substrates (reviewed in Duraisingh and Refour, 2005).

Fluorochromes such as fluorescein acetoxymethylester (AM) derivates have been widely used in imaging and in surrogate assays of P-gp function in normal and malignant cells (Szakacs *et al*, 1998). Fluorescein AM derivates are hydrophobic, cell-permeant substances that only fluoresce after AM hydrolysis by intracellular esterases (Szakacs *et al*, 1998). Cells expressing P-gp expel the nonfluorescent probe, resulting in decreased accumulation of the fluorescent dye in the cytoplasmic compartment (Szakacs *et al*, 1998). As the free fluorochrome is a poor substrate, P-gp transport activity can be quantitatively assessed by measuring the net accumu-

*Corresponding author. Hygiene Institut, Abteilung Parasitologie, Universitätsklinikum Heidelberg, Im Neuenheimer Feld 324, 69120 Heidelberg, Germany. Tel.: +49 6221 567845; Fax: +49 6221 564643; E-mail: michael_lanzer@med.uni-heidelberg.de

Received: 12 January 2006; accepted: 29 May 2006; published online: 22 June 2006

lation of intracellular fluorescence, thereby providing information regarding P-gp protein levels and the directionality of transport (Szakacs *et al*, 1998). Here, we present genetic, positional cloning and pharmacological evidence suggesting that Pgh-1 mediates solute import into, as opposed to solute efflux from, the food vacuole. Moreover, our data suggest that the Fluo-4 staining pattern provides a live cell surrogate assay for Pgh-1 variants associated with altered drug responses.

Results

Clonal variation in Fluo-4 live cell imaging

Figure 1A depicts fluorescent images of different *P. falciparum* parasites loaded with Fluo-4 AM under standardized conditions. While the Dd2, K1 and FCB parasites showed a bright Fluo-4 fluorescence in the food vacuole and a weak fluorescence in the cytoplasm, the HB3, NF54 and 7G8 parasites revealed a distinctly more diffuse staining pattern of the entire parasite. The acidic food vacuole of the parasite was localized using the acidotropic dye LysoSensor Blue DND-192 (LS Blue) (Wissing *et al*, 2002; Rohrbach *et al*, 2005). The clonal variations in Fluo-4 staining were confirmed by quantifying the fluorescence intensities in the food vacuole and cytoplasm (Figure 1B). Both values differed significantly between the two sets of parasites, with Dd2, K1 and FCB having higher food vacuolar and lower cytoplasmic Fluo-4 fluorescence as compared to HB3, NF54 and 7G8. Accordingly, the ratio of the food vacuolar over cytoplasmic fluorescence ($R_{vac/cyt}$) differed two- to three-fold between these two sets of parasites (Figure 1C).

As Fluo-4 fluorescence is calcium-dependent, with the fluorescence increasing with rising free calcium concentrations ($[Ca^{2+}]_i$), we wondered whether the differences observed in Fluo-4 live cell imaging were due to variations in intracellular Ca^{2+} homeostasis. Since Fluo-4 is a nonratiometric Ca^{2+} indicator, calibrating the fluorescence signals is difficult. In a previous study, we used the ratiometric fluorophore Fura-Red AM to quantify free $[Ca^{2+}]_i$ in different subcellular compartments of the parasite and observed that Fura-Red, in a confocal setting, provided reliable and robust recordings of both steady-state and dynamic free $[Ca^{2+}]_i$ (Rohrbach *et al*, 2005). We applied this method to a representative number of parasites. No significant differences in cytoplasmic or food vacuolar free $[Ca^{2+}]_i$ were found between the examined parasites Dd2, K1, HB3 and NF54 ($P > 0.05$) (Table I). The free $[Ca^{2+}]_i$ values measured were consistent with previous determinations (Biagini *et al*, 2003, 2005; Rohrbach *et al*, 2005).

Genetic linkage of the Fluo-4 phenotype to pfmdr1

We next investigated the Fluo-4 fluorescence pattern in 16 genetically distinct progeny from a cross between Dd2 and HB3 (Wellems *et al*, 1990; Su *et al*, 1999) (Figure 2A). Quantitative trait locus (QTL) analysis revealed a locus on chromosome 5, with the highest LOD score of >6 associated with the *pfmdr1* marker (Figure 2B). In fact, all progeny that displayed an intense food vacuolar Fluo-4 staining phenotype contained the Dd2 *pfmdr1* allele (Y^{86}, Y^{184}, S^{1034}, N^{1042} and D^{1246}), whereas progeny with a diffuse Fluo-4 staining inherited the HB3 *pfmdr1* allele (N^{86}, F^{184}, S^{1034}, D^{1042} and D^{1246}) (Figure 2A). To assess the possible linkage with other loci, a secondary scan was performed with the effect of *pfmdr1* removed. No other significant QTL was found (Figure 2C).

To investigate whether *pfmdr1* itself plays a role in the Fluo-4 phenotype, we examined the effect of established P-gp inhibitors on the subcellular Fluo-4 fluorescence pattern. For Dd2, addition of P-gp inhibitors before and during loading with Fluo-4 AM significantly altered the Fluo-4 fluorescence pattern. The preferential staining of the food vacuole over the cytoplasm was substantially reduced in the presence of cyclosporine A (CSA, 10 μM), a first generation P-gp inhibitor, and was completely ablated in the presence of the third generation P-gp inhibitors ONT-093 (ONT, 1 and 10 μM) and XR-9576 (XR, 3 nM and 3 μM) (Figure 3A and B). In the case of XR-9576, a concentration of as low as 3 nM sufficed to render the Fluo-4 fluorescence image similar to that of HB3. Verapamil (VP, 30 μM) did not significantly affect the Fluo-4 staining pattern (Figure 3A and B). For HB3, P-gp inhibitors had no significant effect on the Fluo-4 staining pattern (Figure 3B) and a diffuse staining of the entire parasite remained.

Pgh-1 overexpression enhances food vacuolar Fluo-4 staining

The *pfmdr1* loci of HB3 and Dd2 differ not only regarding polymorphisms (see above) but also regarding copy number (1 versus 3–4, respectively). Taking this into account, we found that the food vacuolar phenotype, in addition to being linked with the Dd2 *pfmdr1* allele, was further associated with an increased *pfmdr1* copy number in the progeny of the HB3 × Dd2 cross (Figure 4A), with the exception of TC08, which contains only one *pfmdr1* gene. Using quantitative real-time PCR, we generally confirmed the published *pfmdr1* copy numbers (Wellems *et al*, 1990), although quantitative real-time PCR indicated lower values for B1SD, 3BB1 and Dd2 (Figure 4A, Supplementary Table I).

The correlation between *pfmdr1* copy number and the Fluo-4 phenotype improved when directly assessing the Pgh-1 protein level. Pgh-1 amounts were quantified by Western analysis, normalized against α-tubulin and expressed in relation to the Pgh-1 level of HB3. All progeny with a diffuse Fluo-4 staining pattern contained the HB3 *pfmdr1* allele and had Pgh-1 protein levels comparable to that of HB3, whereas all progeny with a bright food vacuolar staining contained the Dd2 *pfmdr1* allele and had 1.5- to 3.0-fold higher Pgh-1 protein levels, including TC08 (Figure 4B, Supplementary Table I).

To better assess the contribution of Pgh-1 protein levels to the Fluo-4 phenotype, we examined the parasite FCB and its isogenic clone $KD1^{mdr1}$, in which one of the two *pfmdr1* gene copies present were destroyed by insertional knockout mutagenesis (Sidhu *et al*, in press). Both FCB and $KD1^{mdr1}$ contain the Y^{86}, Y^{184}, S^{1034}, N^{1042} and D^{1246} allelic form of *pfmdr1*, also present in Dd2. FCB revealed a Pgh-1 protein level of 1.8 ± 0.3 (in reference to that of HB3) and a food vacuolar staining phenotype with a high Fluo-4 $R_{vac/cyt}$ value of 3.2 ± 0.1 (Figure 4C and D). In $KD1^{mdr1}$, the Pgh-1 protein level was reduced to 0.9 ± 0.1 and the Fluo-4 $R_{vac/cyt}$ value to 2.2 ± 0.1, yet the food vacuolar staining phenotype remained (Figure 4C and D). This finding suggests that Pgh-1 levels contribute to the extent of the food vacuolar Fluo-4 staining by increasing the Fluo-4 $R_{vac/cyt}$ values. However, Pgh-1 levels do not determine the Fluo-4 staining phenotype, as parasites

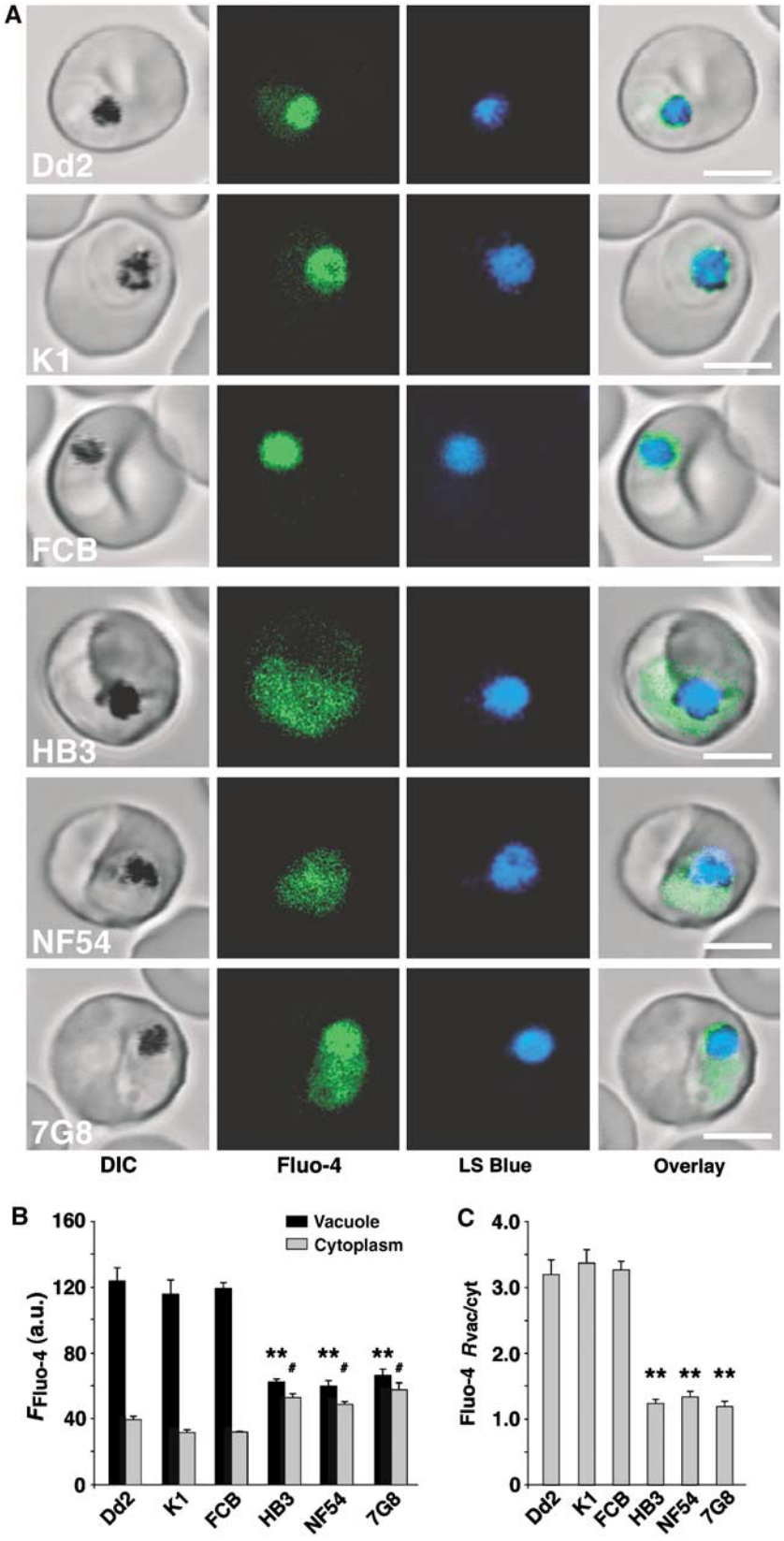

Figure 1 Fluo-4 fluorescence in different *P. falciparum* parasites. (**A**) Single images of *P. falciparum*-infected erythrocytes stained with Fluo-4 AM (green) and the acidotropic dye LS Blue (blue). Bar, 5 μm. (**B**) Mean Fluo-4 fluorescence quantified from the food vacuolar and cytoplasmic regions. (**C**) Ratios of the mean Fluo-4 fluorescence signals in the vacuolar and cytoplasmic regions ($R_{vac/cyt}$). The means ± s.e. of over 15 independent determinations collected over several days are shown in (B) and (C). $^{**}P<0.001$ and $^{\#}P<0.05$, comparing the vacuole and cytoplasm of the two groups of parasites, respectively.

Table I Steady-state free food vacuolar and cytoplasmic $[Ca^{2+}]_i$ in different *P. falciparum* parasites

Parasite	Vacuolar $[Ca^{2+}]_i$ (nM)	Cytoplasmic $[Ca^{2+}]_i$ (nM)
Dd2	454±60 ($n=54$)	352±42 ($n=73$)
K1	375±57 ($n=46$)	289±39 ($n=45$)
HB3	450±52 ($n=64$)	397±34 ($n=81$)
NF54	441±91 ($n=23$)	302±29 ($n=40$)

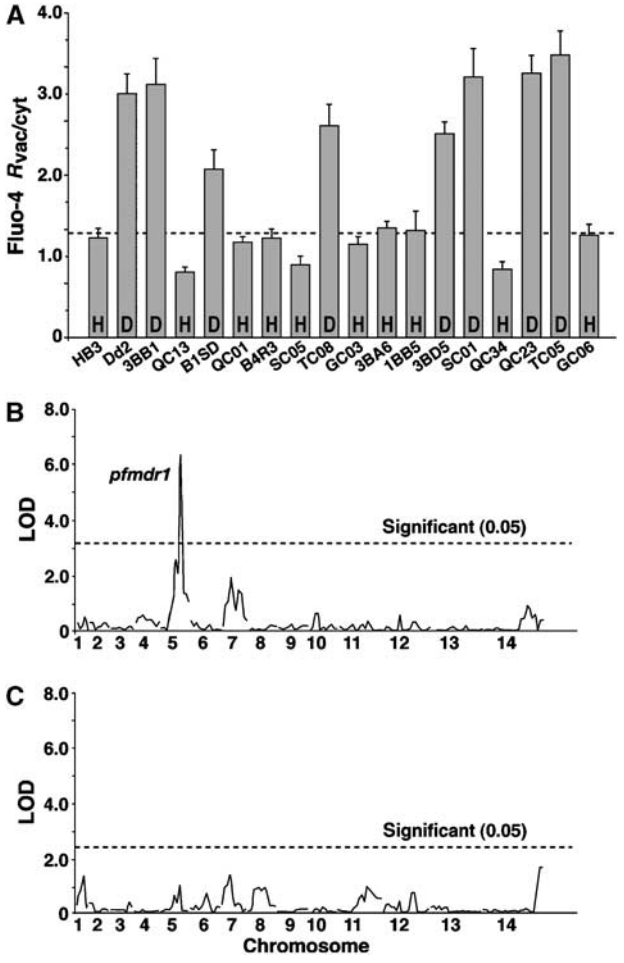

Figure 2 Linkage of the Fluo-4 phenotype to *pfmdr1*. (**A**) Fluo-4 $R_{vac/cyt}$ in the progeny from the HB3 × Dd2 cross. The dotted line indicates the cutoff level of fluorescence ratio, as defined by HB3. H and D indicate the *pfmdr1* haplotypes of HB3 and Dd2, respectively. The mean±s.e. of over 60 independent determinations are shown. (**B**) QTL analysis of Fluo-4 $R_{vac/cyt}$ using Pseudomaker. (**C**) Secondary scan using Pseudomaker to search for minor QTL. Dashed lines represent the threshold values calculated from 1000 permutations (Churchill and Doerge, 1994). The *P. falciparum* chromosomes are indicated.

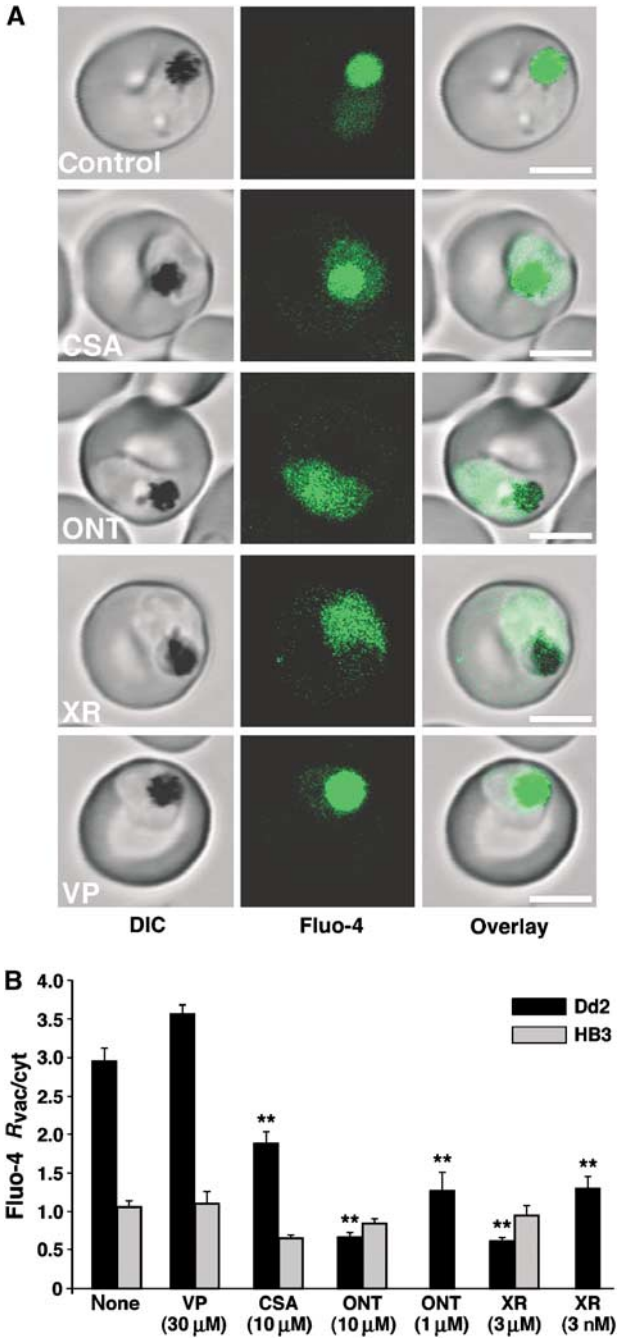

Figure 3 Confocal Fluo-4 AM imaging of vacuolar and cytosolic fluorescence in *P. falciparum* in the presence of various inhibitors. (**A**) Images of Dd2 parasites were obtained after loading with Fluo-4 AM in the presence of the P-gp inhibitors CSA, ONT-093 (ONT), XR-9576 (XR) or verapamil (VP). Bar, 5 μm. (**B**) Ratio of the vacuolar and cytosolic fluorescence (Fluo-4 $R_{vac/cyt}$) measured in Dd2 and HB3 in the presence of various P-gp inhibitors. The concentrations used are indicated. The mean±s.e. of over 10 independent determinations are shown. $^{**}P<0.001$.

with comparable low levels of Pgh-1 can have different Fluo-4 staining patterns (compare $KD1^{mdr1}$ and K1 with HB3 in Supplementary Table I).

The Fluo-4 phenotype is linked with pfmdr1 polymorphisms

We next examined genetically engineered mutants of *pfmdr1* (Reed *et al*, 2000; Sidhu *et al*, 2005), which encode amino-acid substitutions in positions 86, 184, 1034, 1042 and 1246 that have been associated with various drug responses. These include *pfmdr1* mutants generated from GC03 and 3BA6, which are both progeny of the HB3 × Dd2 cross and which share the same *pfmdr1* allele as HB3 (N^{86}, F^{184}, S^{1034}, D^{1042} and D^{1246}). GC03, 3BA6 and their corresponding recombinant controls SDD^{GC03} and SDD^{3BA6} that retain the original HB3

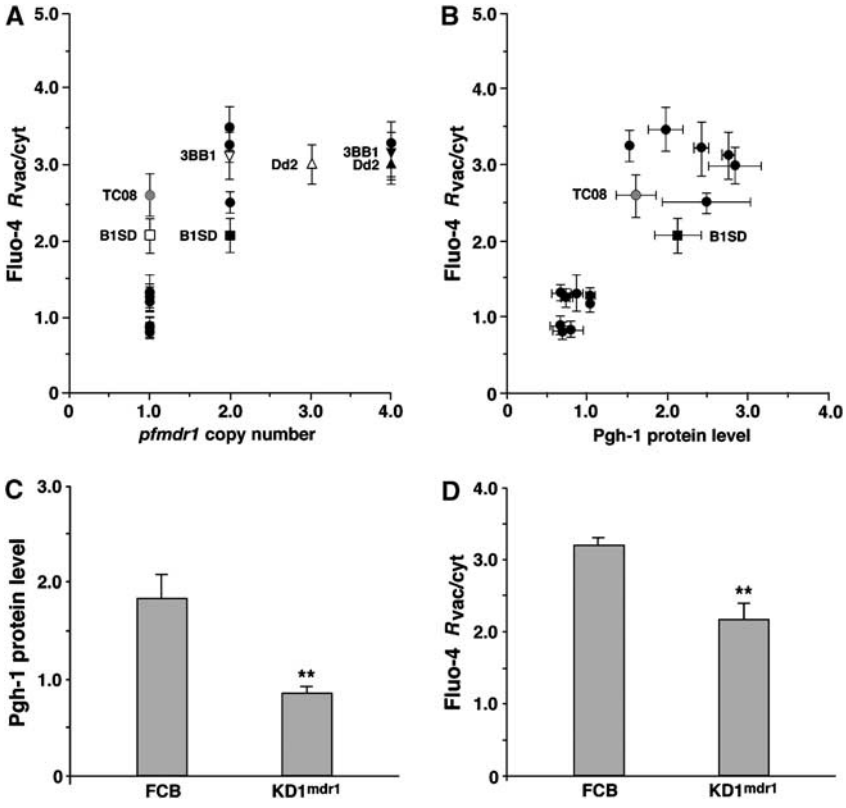

Figure 4 *pfmdr1* overexpression contributes to the food vacuolar Fluo-4 phenotype. (**A**) The *pfmdr1* copy number of the progeny, analyzed as a function of Fluo-4 $R_{vac/cyt}$. The solid circles represent copy numbers that are in agreement using both real-time PCR and Southern analysis. For Dd2, 3BB1 and B1SD, diverging results were obtained (solid triangles and solid squares, Southern analysis; corresponding open symbols, real-time PCR). TC08 (grey circle) represents a clone that harbors one *pfmdr1* gene copy number measured in both methods, yet shows a high Fluo-4 $R_{vac/cyt}$ ratio. (**B**) Pgh-1 protein levels analyzed as a function of Fluo-4 $R_{vac/cyt}$ values. Symbols are as in (A). (**C**) Pgh-1 protein levels evaluated in FCB (harboring two *pfmdr1* gene copies) and its isogenic clone KD1^{mdr1} (harboring one *pfmdr1* copy). (**D**) Fluo-4 $R_{vac/cyt}$ ratios quantified in FCB and KD1^{mdr1}. Means$\pm$s.e. of over 40 independent determinations collected over several days are shown. $^{**}P<0.001$.

pfmdr1 allele revealed the diffuse Fluo-4 staining phenotype of HB3 and a similarly low $R_{vac/cyt}$ value (Figure 5A). The clones SND^{GC03} and SND^{3BA6}, which no longer harbor the N^{1042}D polymorphism in Pgh-1, showed the food vacuolar Fluo-4 phenotype and a significantly higher $R_{vac/cyt}$ value (Figure 5A). The clones CDY^{GC03} and CDY^{3BA6}, which encode the three C-terminal polymorphisms S^{1034}C, N^{1042}D and D^{1246}Y, revealed the diffuse Fluo-4 staining pattern of HB3, albeit their Fluo-4 $R_{vac/cyt}$ values were significantly lower than those of the parental clones GC03 and 3BA6 (Figure 5A).

We also examined *pfmdr1* mutants engineered in D10 and 7G8 parasites. The *pfmdr1* allele of 7G8 encodes four amino-acid substitutions with respect to that of D10: Y^{184}F, S^{1034}C, N^{1042}D, and D^{1246}Y (Supplementary Table II). The allelic exchange mutants investigated were D10-mdr^{D10}, which retained the wild-type D10 *pfmdr1* sequence; D10-mdr$^{7G8/3}$ encoding the S^{1034}C, N^{1042}D, and D^{1246}Y substitutions; D10-mdr$^{7G8/1}$ encoding only the D^{1246}Y substitution; 7G8-mdr^{7G8}, which retained the *pfmdr1* allele of 7G8; and 7G8-mdr^{D10} encoding F^{184}, S^{1034}, N^{1042} and D^{1246} residues. Only 7G8-mdr^{D10} exhibited the food vacuolar Fluo-4 staining phenotype with a high Fluo-4 $R_{vac/cyt}$ value of 2.6$\pm$0.2 (Figure 5A), whereas all other mutants revealed the diffuse Fluo-4 staining pattern with low Fluo-4 $R_{vac/cyt}$ values of approximately 1.0 (Figure 5A), comparable to that of the parental clones D10 and 7G8. Interestingly, 7G8-mdr^{D10}, SND^{GC03} and SND^{3BA6}, which all displayed elevated Fluo-4 $R_{vac/cyt}$ values, encode the same polymorphisms in *pfmdr1*, namely N^{86}, F^{184}, S^{1034}, N^{1042}, D^{1246}.

As controls we investigated previously described *pfcrt* allelic exchange mutants that have a GC03 background and that encode different *pfcrt* alleles found in chloroquine resistant parasites (Sidhu *et al*, 2002). No significant changes in the Fluo-4 staining phenotype were observed as compared to the parental clone GC03 (Figure 5B). This finding was in agreement with the QTL analysis that did not reveal significant linkage of the Fluo-4 phenotype with polymorphisms within *pfcrt* (present on chromosome 7; Figure 2C).

Substrate specificity of Pgh-1 and competition of Fluo-4 accumulation by antimalarial drugs

When erythrocytes infected with Dd2 were incubated with Fluo-4 salt instead of Fluo-4 AM, no fluorescence was observed in the parasite's cytoplasm or food vacuole (Figure 6A). This finding is consistent with the membrane-impermeable nature of the dye (Gee *et al*, 2000). However, in saponin and digitonin permeabilized Dd2 infected erythrocytes (Saliba *et al*, 2003), a strong fluorescence was seen in the food vacuole using both Fluo-4 salt and Fluo-4 AM (Figure 6B). The food vacuolar fluorescence depended on the addition of 2 mM ATP (in the case of the membrane permeable Fluo-4 AM fluorescence increased seven-fold), and could

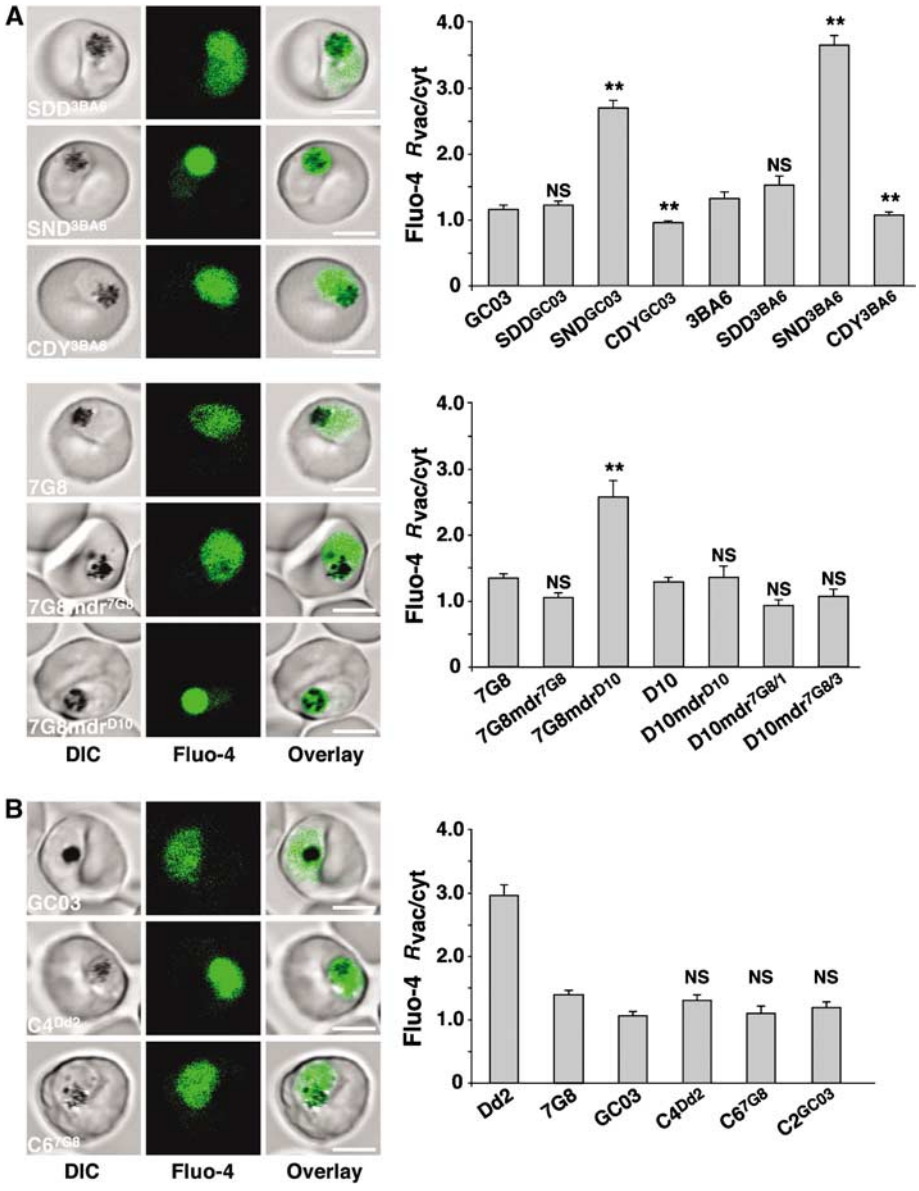

Figure 5 Association of the Fluo-4 phenotype with *pfmdr1* polymorphisms. (**A**) Fluo-4 staining images and ratios of the mean fluorescence signals in the vacuolar and cytoplasmic regions (Fluo-4 $R_{vac/cyt}$), observed in different *pfmdr1* allelic exchange mutants generated on either a GC03, 3BA6, 7G8 or a D10 genetic background (Reed *et al*, 2000; Sidhu *et al*, 2005; Supplementary Table II). NS, not significant as compared to GC03, 3BA6, 7G8 or D10. Means ± s.e. of over 12 independent determinations collected over several days are shown. (**B**) Fluo-4 staining images and Fluo-4 $R_{vac/cyt}$ ratios observed in different *pfcrt* allelic exchange mutants (Sidhu *et al*, 2002). $C4^{Dd2}$ and $C6^{7G8}$ contain the Southeast Asian/African and Latin American *pfcrt* alleles from Dd2 and 7G8, respectively (Sidhu *et al*, 2002). GC03 is the parental clone and $C2^{GC03}$ is a control retaining the *pfcrt* allele of GC03. NS, not significant (compared to GC03). The means ± s.e. of over 14 independent determinations collected over several days are shown. $^{**}P<0.001$; NS, not significant. Bar, 5 μm.

be inhibited by XR-9576 (3 μM) as shown for Fluo-4 salt (Figure 6B). Cell permeability was verified using trypan blue, which stained the cytosol of permeabilized cells but was excluded from the food vacuole under the experimental conditions used (data not shown).

We tested whether Fluo-4 fluorescence was affected by the presence of antimalarial drugs implicated as potential Pgh-1 substrates. For this, we incubated infected erythrocytes with 5 μM Fluo-4 AM and 100 nM of chloroquine, mefloquine, halofantrine, quinine or artemisinin, corresponding to a 50-fold excess of Fluo-4 AM. The Fluo-4 AM concentration was kept at 5 μM to maintain experimental consistency throughout the study. In HB3 and 3BA6, the Fluo-4 fluorescence was unaffected by the addition of these antimalarial drugs (Figure 6C). In comparison, significant decreases in Fluo-4 $R_{vac/cyt}$ values were observed for Dd2 and SND^{3BA6} parasites in the presence of mefloquine, halofantrine, quinine or artemisinin (the latter was only tested for Dd2 and HB3), whereas no significant change occurred in the presence of chloroquine (Figure 6C). To validate this finding, we selected quinine and tested different concentrations ranging from 0 to 500 nM. The Fluo-4 $R_{vac/cyt}$ value responded to increasing concentrations of quinine in Dd2, but not in HB3 (Figure 6D).

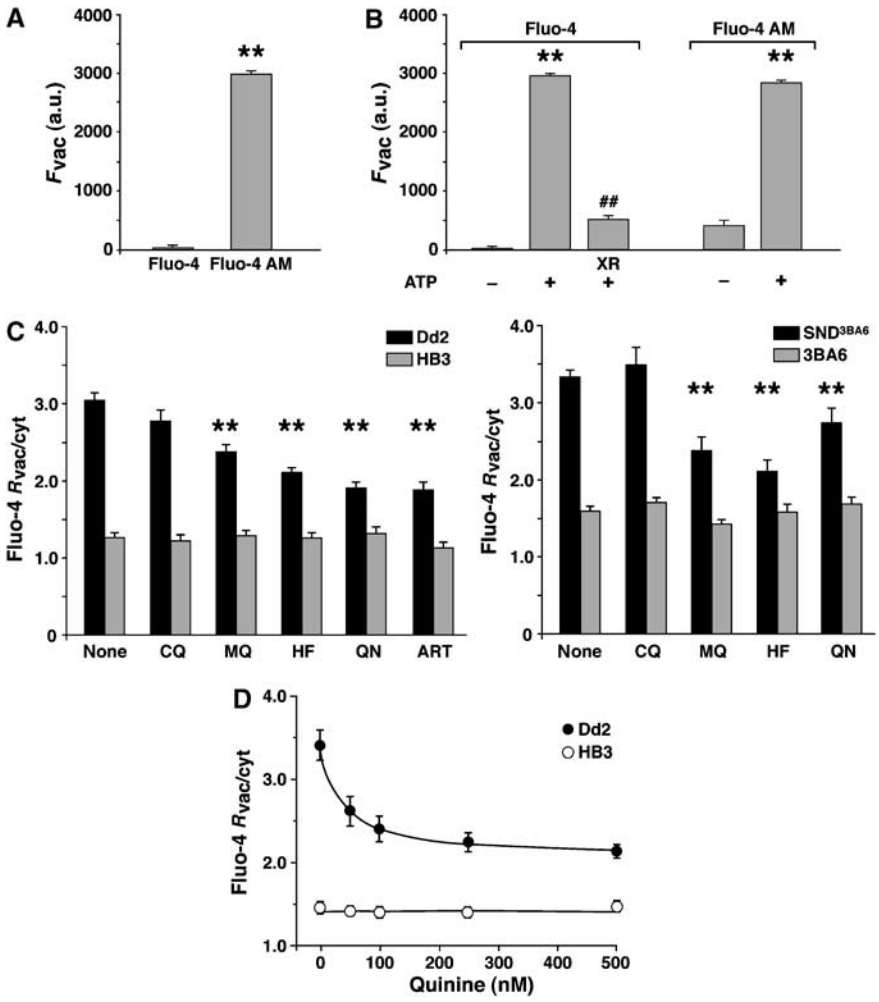

Figure 6 Substrate specificity of Pgh-1. (**A**) Food vacuolar fluorescence of intact erythrocytes infected with Dd2 after incubation with the membrane impermeable fluorochrome Fluo-4 salt and the membrane permeable variant Fluo-4 AM. Means ± s.e. of over 15 independent determinations are shown. a.u., arbitrary units. $^{**}P<0.001$. (**B**) Food vacuolar fluorescence of permeabilized erythrocytes infected with Dd2 using Fluo-4 salt and Fluo-4 AM in the presence and absence of 2 mM ATP. Where indicated XR-9576 (3 μM) was added. Means ± s.e. of over 20 independent determinations are shown. $^{**}P<0.001$ without and with ATP; $^{\#\#}P<0.001$ without and with XR-9576. (**C**) Competition of food vacuolar Fluo-4 fluorescence with different antimalarial drugs. Erythrocytes infected with either Dd2 or HB3 or the *pfmdr1* allelic exchange mutant SND^{3BA6} and its parental clone 3BA6 were incubated with Fluo-4 AM (5 μM) in the presence of 100 nM of chloroquine (CQ), mefloquine (MQ), halofantrine (HF), quinine (QN) or artemisinin (ART) and Fluo-4 $R_{vac/cyt}$ ratios were determined. Means ± s.e. of over 20 independent determinations are shown. $^{**}P<0.001$. (**D**) Erythrocytes infected with Dd2 or HB3 were incubated with Fluo-4 AM (5 μM) and increasing concentrations of quinine and the Fluo-4 $R_{vac/cyt}$ ratios were determined. Means ± s.e. of over 20 independent determinations are shown.

Discussion

We have identified and characterized two distinct Fluo-4 staining phenotypes in *P. falciparum*-infected erythrocytes. Some parasites, including HB3, showed a diffuse fluorescence of the entire parasite, whereas other parasites, such as Dd2, revealed an intense Fluo-4 staining of the food vacuole and only a weak cytoplasmic fluorescence (Figure 1).

As Fluo-4 is a non-ratiometric Ca^{2+} indicator, we considered the possibility that the differences in Fluo-4 staining patterns reflect strain variations in Ca^{2+} homeostasis. However, no significant differences in food vacuolar or cytoplasmic free Ca^{2+} concentrations were observed in the four representative parasites investigated. Our quantitative Ca^{2+} determinations relied on Fura-Red AM, a ratiometric Ca^{2+} indicator that provides reliable recordings of steady-state free $[Ca^{2+}]_i$ in different subcellular compartments of *P. falciparum*-infected erythrocytes (Rohrbach *et al*, 2005). The steady-state food vacuolar and cytoplasmic free $[Ca^{2+}]_i$ values reported herein are consistent with previous determinations (Biagini *et al*, 2003, 2005; Rohrbach *et al*, 2005).

The fluorescence intensity of Fluo-4, unlike that of Fura-Red, is pH sensitive (Rohrbach *et al*, 2005). There are reports suggesting differences in the standing food vacuolar pH between HB3 and Dd2 of 5.7 and 5.2, respectively (Dzekunov *et al*, 2000; Bennett *et al*, 2004), although these studies have been controversial (Bray *et al*, 2002; Wissing *et al*, 2002; Hayward *et al*, 2006). Even if these food vacuolar pH values are considered, this cannot explain the two-fold higher food vacuolar Fluo-4 fluorescence of Dd2. In the acidic range up to pH 6.0, the Fluo-4 fluorescence intensity increases with pH (Rohrbach *et al*, 2005), thus predicting a lower food vacuolar fluorescence for Dd2, which is contrary to our observation.

An alternative model to explain the Fluo-4 phenotypes involves altered fluorochrome handling. Fluo-4 belongs to a group of structurally related fluorescein derivatives that, when present as AM, are known substrates of multidrug efflux systems (Homolya *et al*, 1993; Brezden *et al*, 1994; Nelson *et al*, 1998; Szakacs *et al*, 1998) (Figure 7A). Our finding that, in Dd2, the Fluo-4 staining pattern responded to several established P-gp inhibitors, yielding a staining pattern similar to that of HB3, provided evidence for mechanistic similarities to dye transport in tumor cells. The very characteristic pharmacological profile—partially sensitive to CSA and highly sensitive to the third generation P-gp inhibitors ONT-093 and XR-9576 at concentrations as low as 3 nM (for XR-9576)—suggests that the proposed carrier belongs to the family of multidrug resistance transporters. The observed segregation of the Fluo-4 staining phenotype with *pfmdr1* in the genetic cross between HB3 and Dd2 supports this model. The LOD score of >6 suggests strong linkage with *pfmdr1*. Indeed, all progeny displaying a food vacuolar staining phenotype have the Dd2 *pfmdr1* allele whereas all progeny with a diffuse staining pattern inherited the HB3 *pfmdr1* allele. Although verapamil, at a concentration of 30 μM and within a 40 min incubation time, did not affect the Fluo-4 phenotype, proliferation assays have found that polymorphisms within Pgh-1 can influence the parasite's susceptibility to verapamil (Hayward *et al*, 2005), suggesting a possible interaction between verapamil and Pgh-1.

Investigating several genetically engineered *pfmdr1* mutants confirmed the causative linkage of the food vacuolar Fluo-4 staining phenotype with certain *pfmdr1* polymorphisms. The single amino-acid replacement $D^{1042}N$ within the HB3 *pfmdr1* allele altered the Fluo-4 phenotype of a diffuse to a food vacuolar staining pattern. Similarly, replacing the amino acids $C^{1034}S$, $D^{1042}N$, $Y^{1246}D$ within the *pfmdr1* of 7G8 resulted in a food vacuolar Fluo-4 phenotype from the original diffuse Fluo-4 staining pattern displayed by 7G8. Interestingly, all mutants that have a food vacuolar staining pattern maintain the N^{86}, F^{184}, S^{1034}, N^{1042}, D^{1246} allelic form of *pfmdr1* (Figure 5A). Thus, two allelic forms of *pfmdr1* are associated with a food vacuolar Fluo-4 phenotype, namely Y^{86}, Y^{184}, S^{1034}, N^{1042}, D^{1246} (Dd2, K1 and FCB) and N^{86}, F^{184}, S^{1034}, N^{1042}, D^{1246} (allelic exchange mutants) (Figure 5A). The related allelic form N^{86}, F^{184}, S^{1034}, D^{1042}, D^{1246}, which differs by a single amino-acid substitution at position 1042, replacing the negatively charged aspartic acid by the amide asparagine, showed a diffuse staining pattern. Similarly, a diffuse staining pattern was observed for N^{86}, Y^{184}, S^{1034}, N^{1042}, D^{1246}, which differs by single amino-acid substitutions at positions 86 or 184. This finding suggests a specific interaction with Fluo-4 (Figure 7B). The clones CDY^{GC03} and CDY^{3BA6}, encoding the N^{86}, F^{184}, C^{1034}, D^{1042}, Y^{1246} allelic form of *pfmdr1*, showed an interesting phenotype in that their Fluo-4 $R_{vac/cyt}$ values were significantly lower than those of the parental clones GC03 and 3BA6 or that of HB3 (Figure 5A).

We further noted that the Pgh-1 protein level contributes to the food vacuolar Fluo-4 phenotype. There is a trend towards this effect in the progeny from the genetic cross, which was genetically validated by investigating FCB and its isogenic clone $KD1^{mdr1}$. Disruption of one of the two *pfmdr1* copies decreased Pgh-1 protein level in $KD1^{mdr1}$ and to the same

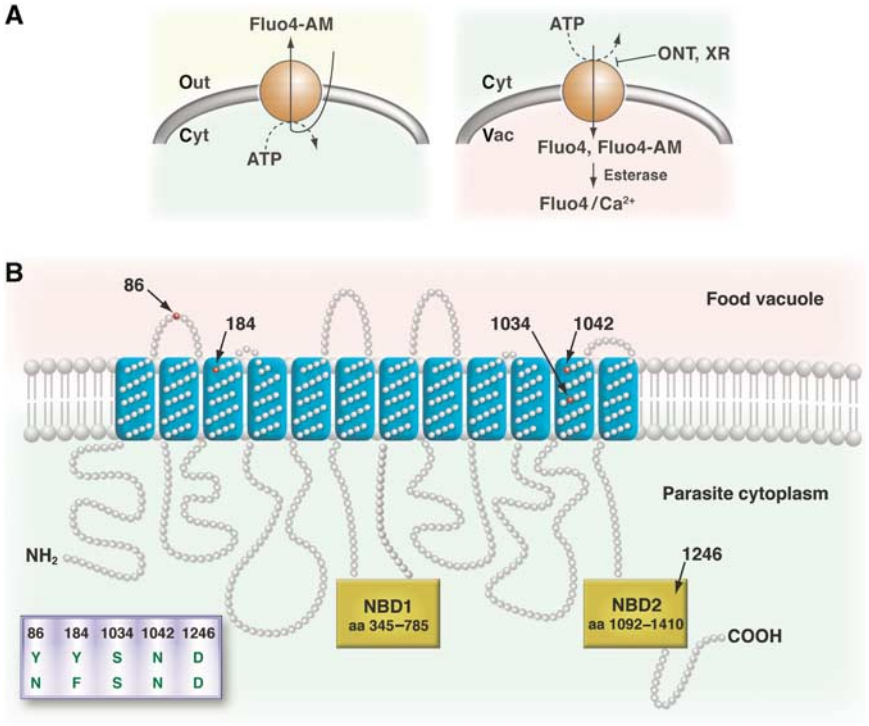

Figure 7 Models of Fluo-4 AM transport in tumor cells and *P. falciparum*. (**A**) Fluo-4 AM passively diffuses through membranes and can be actively extruded by P-gp in tumor cells (left). In parasites, Fluo-4 AM enters by passive diffusion and is converted to the free fluorochrome Fluo-4. Some Pgh-1 variants are capable of pumping both Fluo-4 AM and the membrane impermeable Fluo-4 into the food vacuole. Fluo-4 AM entering the food vacuole is de-esterified by esterases present in this organelle (right) (Krugliak *et al*, 2003). (**B**) Predicted topology of Pgh-1. Polymorphisms associated with both increased Fluo-4 AM/Fluo-4 import into the food vacuole and altered drug responses are indicated. NBD, nucleotide-binding domain.

extent reduced the Fluo-4 $R_{vac/cyt}$ value, albeit the overall staining pattern remained that of a food vacuolar phenotype (Figure 4C and D).

While our data causatively link the Fluo-4 phenotype to *pfmdr1*, there are clear differences to *mdr*-mediated fluorochrome efflux in cancer cells. In tumor cells, P-gp expel the nonfluorescent esterified probe, resulting in reduced intracellular fluorescence (Homolya *et al*, 1993) (Figure 7A, left scheme), while in some *P. falciparum* parasites the fluorochrome accumulates in an intracellular compartment. These apparent differences can be reconciled when the different subcellular localizations of P-gp and Pgh-1 are considered. In tumor cells, P-gp are localized to the plasma membrane, whereas Pgh-1 mainly resides within the parasite's food vacuolar membrane (Cowman *et al*, 1991; Cremer *et al*, 1995). On the basis of these considerations, we propose that Pgh-1, in a variant-dependent manner, pumps solutes into the food vacuole (Figure 7A, right scheme). Inwardly directed transport is fully consistent with the predicted topology of Pgh-1, with its ATP-binding domain facing the cytoplasm (Cowman *et al*, 1991; Karcz *et al*, 1993). Our model is supported by several independent lines of evidence: (i) the food vacuolar phenotype intensified with increasing *pfmdr1* copy number (Figure 4C and D); (ii) Fluo-4 AM, but more importantly, the membrane-impermeable form, Fluo-4 salt, accumulated in the food vacuoles of permeabilized erythrocytes infected with Dd2 in an ATP-dependent manner (Figure 6B); and (iii) accumulation of Fluo-4 salt (permeabilized cells, Figure 6B) and Fluo-4 AM (live cells, Figure 3) could be inhibited by the established P-gp inhibitor XR-9576. While P-gp transports Fluo-4 AM and only poorly the de-esterified form (Szakacs *et al*, 1998), Pgh-1 seems to use both Fluo-4 salt and Fluo-4 AM as substrates.

The conclusion that Pgh-1 can transport solutes into the food vacuole has major implications for the interpretation of antimalarial drug responses. The Pgh-1 variants that most effectively concentrate Fluo-4 salt/Fluo-4 AM in the food vacuole are those that have been linked to reduced susceptibility to artemisinin, halofantrine and mefloquine and increased susceptibility to quinine (Reed *et al*, 2000; Sidhu *et al*, 2005). Conversely, parasites expressing the N^{86}, F^{184}, C^{1034}, D^{1042}, Y^{1246} allelic form of *pfmdr1* concentrate the least Fluo-4 salt/Fluo-4 AM in their food vacuoles and concomitantly have an increased susceptibility to mefloquine, halofantrine and possibly artemisinin (Reed *et al*, 2000; Sidhu *et al*, 2005). Thus, the Fluo-4 staining pattern directly correlates with certain drug responses, providing a rapid cell-based diagnostic assay for *pfmdr1* polymorphisms associated with various drugs. Indeed, accumulation of Fluo-4 into the food vacuole could be competed by mefloquine, halofantrine, quinine and artemisinin, but not chloroquine (Figure 6C). For quinine, a concentration-dependent response was established (Figure 6D), albeit Fluo-4 $R_{vac/cyt}$ values could not be reduced to the level observed in parasites with a diffuse fluorescence staining pattern, possibly because Pgh-1, like human P-gp (Shapiro *et al*, 1999; Shapiro and Ling, 1997), may possess multiple transport-active and substrate-specific binding sites (in this case one for Fluo-4 salt/Fluo-4 AM and one for quinine) that may interact in a cooperative fashion. Chloroquine, a highly acidotropic compound that accumulates in the parasite's food vacuole (Yayon *et al*, 1984), and possibly alkalinizing this compartment (Yayon *et al*, 1985), had no effect on the food vacuolar Fluo-4 fluorescence, providing further evidence for our model that the Fluo-4 staining pattern is unrelated to pH. Our finding that chloroquine does not compete with Fluo-4 in HB3 and Dd2 is consistent with genetic and positional cloning experiments that dissociated chloroquine resistance from the Pgh-1 polymorphisms displayed by HB3 and Dd2 (Wellems *et al*, 1990; Sidhu *et al*, 2005), although other Pgh-1 variant may directly or indirectly interact with chloroquine (Reed *et al*, 2000).

On the basis of these findings, it is tempting to speculate that various forms of Pgh-1 transport several antimalarial drugs into the food vacuole. For mefloquine, halofantrine and artemisinin, it may be advantageous to the parasite to sequester these drugs in a compartment where they are less harmful. Recent evidence of possible cytoplasmic targets for artemisinin is fully consistent with this concept (Eckstein-Ludwig *et al*, 2003). Alternatively, Pgh-1 itself may be the target of antimalarial drugs, as suggested for mefloquine (Rubio and Cowman, 1996). In the case of quinine, its site of action is believed to be the food vacuole (Hawley *et al*, 1998; Mungthin *et al*, 1998) and concentrating the drug in this organelle may be disadvantageous; consequently, *pfmdr1* polymorphisms are selected that mediate reduced drug import. Importantly, the $N^{1042}D$ substitution that has been associated with low-level quinine resistance (Sidhu *et al*, 2005) abrogates accumulation of Fluo-4 in the food vacuole (Figure 5A). In summary, our study provides evidence for Pgh-1 mediated solute import into the parasite's food vacuole in a manner that may involve interactions at several, if not all, polymorphic residues.

Materials and methods

Chemicals and antibodies

Fluo-4 AM, Fluo-4 pentapotassium salt, Fura-Red AM, LysoSensor Blue DND-192, Pluronic F-127, Alexa Fluor 680 goat anti-rabbit IgG and Alexa Fluor goat anti-mouse IgG were purchased from Molecular Probes (Netherlands). The Ca^{2+}-ionophore nigericin was purchased from Calbiochem (Germany). The P-gp inhibitor Cyclosporin A (CSA) was obtained from Sigma (Germany), ONT-093 was kindly supplied by Ontogen and XR-9576 by Xenova. Chloroquine, artemisinin and quinine were purchased from Sigma (Germany), mefloquine from Roche (Germany), and halofantrine from GalaxoSmithKline (UK). α-Tubulin clone B-5-1-2 was purchased from Sigma (Germany) and α-Pgh-1 was a kind gift from A Cowman.

P. falciparum culture

P. falciparum parasites were maintained in continuous *in vitro* cultures (adapted from Trager and Jensen, 1976). Live cell experiments were carried out using synchronized *P. falciparum* trophozoites harvested 28–34 h post invasion.

Dye loading of P. falciparum parasites

Cells were washed twice with Ringer's solution (122.5 mM NaCl, 5.4 mM KCl, 1.2 mM $CaCl_2$, 0.8 mM $MgCl_2$, 11 mM D-glucose, 10 mM HEPES, 1 mM NaH_2PO_4, pH 7.4) and loaded with 5 μM Fluo-4 AM in Ringer's solution with Pluronic F-127 (0.1% v/v) or Fluo-4 for 40 min at 37°C. Dye loaded parasites were settled onto poly-L-lysine coated coverslips in a microperfusion chamber as previously described (Wunsch *et al*, 1998). Unbound parasites and remaining dye were washed away by perfusion with Ringer's solution. For the double labeling experiments, Ringer's solution was supplemented with 1 μM of the fluorescent dye LysoSensor Blue DND-192. The P-gp inhibitors verapamil (30 μM), CSA (10 μM), ONT-093 (10 and 1 μM) and XR-9576 (3 μM and 3 nM) were added to *P. falciparum*-infected erythrocytes 10 min prior to loading with Fluo-4 AM. For the competition assays, 100 nM of the antimalarial drugs

chloroquine, mefloquine, halofantrine, quinine or artemisinin were incubated with 5 μM Fluo-4 AM for 40 min at 37°C.

Selective permeabilization of the erythrocyte and parasite plasma membranes

Infected erythrocytes were permeabilized by brief exposure to saponin (0.01% w/v), permeabilizing both the host cell membrane and the parasitophorous vacuole membrane (Ansorge *et al*, 1997; Saliba *et al*, 2003) and giving extracellular solutes access to the parasite plasma membrane. The plasma membrane of the parasite was permeabilized using digitonin (Krogstad *et al*, 1985), permitting solutes added to the extracellular medium access to the food vacuolar membrane (Saliba *et al*, 2003). Isolated parasites were suspended in 2 ml of ice-cold buffer (110 mM KCl, 30 mM NaCl, 2 mM $MgCl_2$, 5 mM HEPES, pH 7.3). The cell suspension was kept on ice for 5–10 min before adding digitonin (0.02% w/v). The cells were mixed gently and returned to ice for additional 4 min, after which time 1 ml of ice-cold buffer containing 1 mg/ml bovine serum albumin (BSA) was added. The permeabilized parasites were immediately centrifuged (15 800 *g*) for 1 min, washed twice (1 min at 15 800 *g*) with 1 ml of the same BSA-containing solution, and then once in buffer without BSA. Digitonin-permeabilized parasites were suspended in buffer and placed at 37°C until use (within 30 min to 1 h). Permeabilized parasites were loaded with 5 μM of either Fluo-4 AM or Fluo-4, and ATP was supplemented at 2 mM where mentioned. XR-9576 (3 μM) was added to permeabilized erythrocytes, maintained at 37°C, 10 min prior to addition of the fluorochrome.

Live cell imaging

Confocal scanning fluorescence microscopy was performed using a Zeiss LSM510 (Carl Zeiss, Germany) equipped with UV and visible laser lines. Multi-Track mode was used for LysoSensor Blue DND-192 (excited at 364 nm with emission detected using the BP 385–470 nm filter, blue channel) and Fluo-4 AM or Fluo-4 (excited at 488 nm with emission using LP 505 nm filter, green channel). Optimized laser settings were excitation 488 nm with 1% transmission, and 364 nm with 2% transmission. Single images were obtained using a $\times 63$ lens (C-APO, N.A. = 1.2) with an eight-fold software zoom at 512×512 pixel. For Fluo-4 AM (or Fluo-4) labeling alone, Single-Track mode was applied using the above-mentioned laser and filter. Regions of interest restricted to either the vacuole or the cytosol of the parasite were defined and fluorescence intensity quantified, using the LSM510 v3.2 software.

In situ Ca^{2+}-calibration of Fura-Red

The fluorescent calcium indicator Fura-Red AM was used to measure the intracellular free calcium concentration, as described (Rohrbach *et al*, 2005). Mean resting free $[Ca^{2+}]_i$ were compared between the vacuole and the cytoplasmic area using a Student's *t*-test at the $P = 0.05$ level.

Genome-wide scans

The Dd2 × HB3 genetic cross and genetic linkage map have been previously described (Wellems *et al*, 1990; Su *et al*, 1999). QTL linked to Fluo-4 fluorescence were analyzed using Pseudomaker (Sen and Churchill, 2001). Significance thresholds were determined by permutation analyses (Churchill and Doerge, 1994; Lander and Kruglyak, 1995). A secondary scan was used to search for minor QTL (Doerge and Churchill, 1996).

Real-time PCR

pfmdr1 copy number was determined by TaqMan real-time PCR using an ABI 7700. The *pfmdr1* probe was FAM™ (6-carboxy-fluorescein) labeled at the 5′-end, and the α-tubulin probe was VIC™ labeled. Both probes had a TAMRA™ label at the 3′-end. Amplification reactions were carried out in MicroAmp 96-well plates in 25 μl volumes, containing TaqMan buffer, passive reference dye ROX (5-carboxy-X-rhodamine), 300 nM forward and reverse primer, 100 nM of each probe, and 100 ng purified parasite genomic DNA. Forty cycles were performed (95°C for 15 s and at 58°C for 1 min). Fluorescence data were expressed as normalized reporter signals, calculated by dividing the amount of reporter signal by the passive reference signal. The optimal detection threshold was determined for the assay conditions and used for every run. Results were analyzed by a delta–delta C_t method. The assay was replicated four independent times and normalized to HB3, which was included in every run. Primers and probes used were:

pfmdr1^{sense} (TTAAGTTTTACTCTAAAAGAAGGGAAAACATAT);
pfmdr1^{antisense} (TCTCCTTCGGTTGGATCATAAAG);
pfmdr1 probe (CATTTGTGGGAGAATCAGGTTGTGGGAAAT);
α-tubulin^{sense} (TGATGTGCGCAAGTGATCC);
α-tubulin^{antisense} (TCCTTTGTGGACATTCTTCCTC);
α-tubulin probe (TAGCACATGCCGTTAAATATCTTCCATGTCT).

Pgh-1 expression levels

Magnet-purified trophozoite-infected erythrocytes were isolated as described (Sanchez *et al*, 2003). After purification, erythrocytes were lysed by hypotonic shock at 4°C (Herwaldt *et al*, 1990). Protein amounts were determined using Bradford assays (BioRad, Germany). Samples were run on NuPAGE Novex Tris-Acetate gels (Invitrogen, Germany) and transferred onto a 0.2 μm PDVF membrane (BioRad, Germany). Membranes were blocked overnight at 4°C using 5% milk in PBS. Primary antibodies (α-Pgh-1 and α-tubulin, both diluted 1:1000) were incubated for 1 h at RT in 1% BSA/PBS. Membranes were washed three times using PBS/0.1% Tween for 10 min at RT and then blocked again in 5% milk in PBS for 1 h. Secondary antibodies (Alexa Fluor 680 goat anti-rabbit IgG, or Alexa Fluor goat anti-mouse IgG, both diluted 1:10 000) were added to 1% BSA/PBS for 30 min at RT. After washing four times in PBS/0.1% Tween for 5 min at RT, signals were read using an Odyssey-Li-cor infrared imaging system (Li-cor Biosciences). Fluorescence intensities for Pgh-1 were normalized using fluorescence intensities measured for α-tubulin. The resulting values were then expressed in relation to HB3.

Statistical analysis

Statistical significance (*P*-value) was tested using the Student's *t*-test (Sigma Plot, SPSS software).

Online supplemental material

Supplementary Table I shows *pfmdr1* inheritance and copy number in various parasites. Supplementary Table II shows relevant point mutations in Pgh-1.

Supplementary data

Supplementary data are available at *The EMBO Journal* Online.

Acknowledgements

This work was supported by the SFB 544 'Control of Tropical Infectious Diseases' (ML), the European Network of Excellence BioMalPar (ML) and a Blood Disease Research Grant from the New York Community Trust (DF). We thank Anne-Catrin Uhlemann, Sanjeev Krishna and Stephanie Gaw-Volderramos for their contribution to generating and characterizing the *pfmdr1* knockdown lines, as well as Elisabeth Wilken, Marina Müller and Christine Reinhardt for technical help. We are grateful to Tom Wellems for the progeny of the HB3 × Dd2 cross and Alan Cowman for *pfmdr1* allelic exchange mutants and Pgh-1 antiserum.

References

Ansorge I, Paprotka K, Bhakdi S, Lingelbach K (1997) Permeabilization of the erythrocyte membrane with streptolysin O allows access to the vacuolar membrane of *Plasmodium falciparum* and a molecular analysis of membrane topology. *Mol Biochem Parasitol* **84:** 259–261

Baird JK (2005) Effectiveness of antimalarial drugs. *N Engl J Med* **352:** 1565–1577

Bennett TN, Kosar AD, Ursos LM, Dzekunov S, Singh Sidhu AB, Fidock DA, Roepe PD (2004) Drug resistance-associated *pfcrt* mutations confer decreased *Plasmodium falciparum* digestive vacuolar pH. *Mol Biochem Parasitol* **133:** 99–114

Biagini GA, Bray PG, Spiller DG, White MR, Ward SA (2003) The digestive food vacuole of the malaria parasite is a dynamic intracellular Ca2 + store. *J Biol Chem* **278:** 27910–27915

Biagini GA, Fidock DA, Bray PG, Ward SA (2005) Mutations conferring drug resistance in malaria parasite drug transporters Pgh1 and Pfcrt do not affect steady-state vacuolar Ca2+. *Antimicrob Agents Chemother* **49:** 4807–4808

Borges-Walmsley MI, McKeegan KS, Walmsley AR (2003) Structure and function of efflux pumps that confer resistance to drugs. *Biochem J* **376:** 313–338

Bray PG, Saliba KJ, Davies JD, Spiller DG, White MR, Kirk K, Ward SA (2002) Distribution of acridine orange fluorescence in *Plasmodium falciparum*-infected erythrocytes and its implications for the evaluation of digestive vacuole pH. *Mol Biochem Parasitol* **119:** 301–304; discussion 307–309, 311–313

Brezden CB, Hedley DW, Rauth AM (1994) Constitutive expression of P-glycoprotein as a determinant of loading with fluorescent calcium probes. *Cytometry* **17:** 343–348

Churchill GA, Doerge RW (1994) Empirical threshold values for quantitative trait mapping. *Genetics* **138:** 963–971

Cowman AF, Galatis D, Thompson JK (1994) Selection for mefloquine resistance in *Plasmodium falciparum* is linked to amplification of the *pfmdr1* gene and cross-resistance to halofantrine and quinine. *Proc Natl Acad Sci USA* **91:** 1143–1147

Cowman AF, Karcz S, Galatis D, Culvenor JG (1991) A P-glycoprotein homologue of *Plasmodium falciparum* is localized on the digestive vacuole. *J Cell Biol* **113:** 1033–1042

Cremer G, Basco LK, Le Bras J, Camus D, Slomianny C (1995) *Plasmodium falciparum*: detection of P-glycoprotein in chloroquine-susceptible and chloroquine-resistant clones and isolates. *Exp Parasitol* **81:** 1–8

Doerge RW, Churchill GA (1996) Permutation tests for multiple loci affecting a quantitative character. *Genetics* **142:** 285–294

Duraisingh MT, Cowman AF (2005) Contribution of the *pfmdr1* gene to antimalarial drug-resistance. *Acta Trop* **94:** 181–190

Duraisingh MT, Refour P (2005) Multiple drug resistance genes in malaria—from epistasis to epidemiology. *Mol Microbiol* **57:** 874–877

Duraisingh MT, Roper C, Walliker D, Warhurst DC (2000) Increased sensitivity to the antimalarials mefloquine and artemisinin is conferred by mutations in the *pfmdr1* gene of *Plasmodium falciparum*. *Mol Microbiol* **36:** 955–961

Dzekunov SM, Ursos LM, Roepe PD (2000) Digestive vacuolar pH of intact intraerythrocytic *P. falciparum* either sensitive or resistant to chloroquine. *Mol Biochem Parasitol* **110:** 107–124

Eckstein-Ludwig U, Webb RJ, Van Goethem ID, East JM, Lee AG, Kimura M, O'Neill PM, Bray PG, Ward SA, Krishna S (2003) Artemisinins target the SERCA of *Plasmodium falciparum*. *Nature* **424:** 957–961

Foote SJ, Thompson JK, Cowman AF, Kemp DJ (1989) Amplification of the multidrug resistance gene in some chloroquine-resistant isolates of *P. falciparum*. *Cell* **57:** 921–930

Gee KR, Brown KA, Chen WN, Bishop-Stewart J, Gray D, Johnson I (2000) Chemical and physiological characterization of fluo-4 Ca(2+)-indicator dyes. *Cell Calcium* **27:** 97–106

Hawley SR, Bray PG, Mungthin M, Atkinson JD, O'Neill PM, Ward SA (1998) Relationship between antimalarial drug activity, accumulation, and inhibition of heme polymerization in *Plasmodium falciparum in vitro*. *Antimicrob Agents Chemother* **42:** 682–686

Hayward R, Saliba KJ, Kirk K (2005) Mutations in *pfmdr1* modulate the sensitivity of *Plasmodium falciparum* to the intrinsic antiplasmodial activity of verapamil. *Antimicrob Agents Chemother* **49:** 840–842

Hayward R, Saliba KJ, Kirk K (2006) The pH of the digestive vacuole of *Plasmodium falciparum* is not associated with chloroquine resistance. *J Cell Sci* **119:** 1016–1025

Herwaldt BL, Schlesinger PH, Krogstad DJ (1990) Accumulation of chloroquine by membrane preparations from *Plasmodium falciparum*. *Mol Biochem Parasitol* **42:** 257–267

Homolya L, Hollo Z, Germann UA, Pastan I, Gottesman MM, Sarkadi B (1993) Fluorescent cellular indicators are extruded by the multidrug resistance protein. *J Biol Chem* **268:** 21493–21496

Jambou R, Legrand E, Niang M, Khim N, Lim P, Volney B, Ekala MT, Bouchier C, Esterre P, Fandeur T, Mercereau-Puijalon O (2005) Resistance of *Plasmodium falciparum* field isolates to *in-vitro* artemether and point mutations of the SERCA-type PfATPase6. *Lancet* **366:** 1960–1963

Karcz SR, Galatis D, Cowman AF (1993) Nucleotide binding properties of a P-glycoprotein homologue from *Plasmodium falciparum*. *Mol Biochem Parasitol* **58:** 269–276

Krogstad DJ, Schlesinger PH, Gluzman IY (1985) Antimalarials increase vesicle pH in *Plasmodium falciparum*. *J Cell Biol* **101:** 2302–2309

Krugliak M, Zhang J, Nissani E, Steiner-Mordoch S, Ginsburg H (2003) Killing of intraerythrocytic *Plasmodium falciparum* by lysosomotropic amino acid esters. *Parasitol Res* **89:** 451–458

Lander E, Kruglyak L (1995) Genetic dissection of complex traits: guidelines for interpreting and reporting linkage results. *Nat Genet* **11:** 241–247

Mungthin M, Bray PG, Ridley RG, Ward SA (1998) Central role of hemoglobin degradation in mechanisms of action of 4-aminoquinolines, quinoline methanols, and phenanthrene methanols. *Antimicrob Agents Chemother* **42:** 2973–2977

Nelson EJ, Zinkin NT, Hinkle PM (1998) Fluorescence methods to assess multidrug resistance in individual cells. *Cancer Chemother Pharmacol* **42:** 292–299

Ngo T, Duraisingh M, Reed M, Hipgrave D, Biggs B, Cowman AF (2003) Analysis of *pfcrt*, *pfmdr1*, *dhfr*, and *dhps* mutations and drug sensitivities in *Plasmodium falciparum* isolates from patients in Vietnam before and after treatment with artemisinin. *Am J Trop Med Hyg* **68:** 350–356

Pickard AL, Wongsrichanalai C, Purfield A, Kamwendo D, Emery K, Zalewski C, Kawamoto F, Miller RS, Meshnick SR (2003) Resistance to antimalarials in Southeast Asia and genetic polymorphisms in *pfmdr1*. *Antimicrob Agents Chemother* **47:** 2418–2423

Price RN, Uhlemann AC, Brockman A, McGready R, Ashley E, Phaipun L, Patel R, Laing K, Looareesuwan S, White NJ, Nosten F, Krishna S (2004) Mefloquine resistance in *Plasmodium falciparum* and increased *pfmdr1* gene copy number. *Lancet* **364:** 438–447

Reed MB, Saliba KJ, Caruana SR, Kirk K, Cowman AF (2000) Pgh1 modulates sensitivity and resistance to multiple antimalarials in *Plasmodium falciparum*. *Nature* **403:** 906–909

Rohrbach P, Friedrich O, Hentschel J, Plattner H, Fink RH, Lanzer M (2005) Quantitative calcium measurements in subcellular compartments of *P. falciparum*-infected erythrocytes. *J Biol Chem* **280:** 27960–27969

Rubio JP, Cowman AF (1996) The ATP-binding cassette (ABC) gene family of *Plasmodium falciparum*. *Parasitol Today* **12:** 135–140

Saliba KJ, Allen RJ, Zissis S, Bray PG, Ward SA, Kirk K (2003) Acidification of the malaria parasite's digestive vacuole by a H+-ATPase and a H+-pyrophosphatase. *J Biol Chem* **278:** 5605–5612

Sanchez CP, Stein W, Lanzer M (2003) Trans stimulation provides evidence for a drug efflux carrier as the mechanism of chloroquine resistance in *Plasmodium falciparum*. *Biochemistry* **42:** 9383–9394

Sen S, Churchill GA (2001) A statistical framework for quantitative trait mapping. *Genetics* **159:** 371–387

Shapiro AB, Fox K, Lam P, Ling V (1999) Stimulation of P-glycoprotein-mediated drug transport by prazosin and progesterone. Evidence for a third drug-binding site. *Eur J Biochem* **259:** 841–850

Shapiro AB, Ling V (1997) Positively cooperative sites for drug transport by P-glycoprotein with distinct drug specificities. *Eur J Biochem* **250:** 130–137

Sidhu ABS, Uhlemann A-C, Valderramos SG, Valderramos J-C, Krishna S, Fidock DA (2006) Decreasing *pfmdr1* copy number in *Plasmodium falciparum* heightens sensitivity to mefloquine, lumefantrine, halofantrine, quinine and artemisinin. *Journal Infect Dis* (in press)

Sidhu AB, Valderramos SG, Fidock DA (2005) *pfmdr1* mutations contribute to quinine resistance and enhance mefloquine and artemisinin sensitivity in *Plasmodium falciparum*. *Mol Microbiol* **57:** 913–926

Sidhu AB, Verdier-Pinard D, Fidock DA (2002) Chloroquine resistance in *Plasmodium falciparum* malaria parasites conferred by *pfcrt* mutations. *Science* **298:** 210–213

Sisowath C, Stromberg J, Martensson A, Msellem M, Obondo C, Bjorkman A, Gil JP (2005) *In vivo* selection of *Plasmodium falciparum pfmdr1* 86N coding alleles by artemether-lumefantrine (Coartem). *J Infect Dis* **191:** 1014–1017

Snow RW, Guerra CA, Noor AM, Myint HY, Hay SI (2005) The global distribution of clinical episodes of *Plasmodium falciparum* malaria. *Nature* **434:** 214–217

Su X, Ferdig MT, Huang Y, Huynh CQ, Liu A, You J, Wootton JC, Wellems TE (1999) A genetic map and recombination parameters of the human malaria parasite *Plasmodium falciparum*. *Science* **286:** 1351–1353

Szakacs G, Jakab K, Antal F, Sarkadi B (1998) Diagnostics of multidrug resistance in cancer. *Pathol Oncol Res* **4:** 251–257

Trager W, Jensen JB (1976) Human malaria parasites in continuous culture. *Science* **193:** 673–675

Wellems TE, Panton LJ, Gluzman IY, do Rosario VE, Gwadz RW, Walker-Jonah A, Krogstad DJ (1990) Chloroquine resistance not linked to *mdr*-like genes in a *Plasmodium falciparum* cross. *Nature* **345:** 253–255

Wilson CM, Serrano AE, Wasley A, Bogenschutz MP, Shankar AH, Wirth DF (1989) Amplification of a gene related to mammalian *mdr* genes in drug-resistant *Plasmodium falciparum*. *Science* **244:** 1184–1186

Wilson CM, Volkman SK, Thaithong S, Martin RK, Kyle DE, Milhous WK, Wirth DF (1993) Amplification of *pfmdr* 1 associated with mefloquine and halofantrine resistance in *Plasmodium falciparum* from Thailand. *Mol Biochem Parasitol* **57:** 151–160

Wissing F, Sanchez CP, Rohrbach P, Ricken S, Lanzer M (2002) Illumination of the malaria parasite *Plasmodium falciparum* alters intracellular pH. Implications for live cell imaging. *J Biol Chem* **277:** 37747–37755

Wunsch S, Sanchez CP, Gekle M, Grosse-Wortmann L, Wiesner J, Lanzer M (1998) Differential stimulation of the Na+/H+ exchanger determines chloroquine uptake in *Plasmodium falciparum*. *J Cell Biol* **140:** 335–345

Yayon A, Cabantchik ZI, Ginsburg H (1984) Identification of the acidic compartment of *Plasmodium falciparum*-infected human erythrocytes as the target of the antimalarial drug chloroquine. *EMBO J* **3:** 2695–2700

Yayon A, Cabantchik ZI, Ginsburg H (1985) Susceptibility of human malaria parasites to chloroquine is pH dependent. *Proc Natl Acad Sci USA* **82:** 2784–2788